AN EXPERIMENTAL INVESTIGATION OF THERMAL LOADING ON A PLATE FROM PARALLEL TRIPLE JET

Paul J. Kristo[1], D. Tyler Landfried[1] and Mark L. Kimber[2]
[1]Department of Mechanical Engineering and Material Science, University of Pittsburgh
3700 O'Hara St, Pittsburgh, PA 15213, USA
pjk26@pitt.edu, dtl5@pitt.edu

[2]Assistant Professor, Department of Mechanical Engineering and Material Science
Benedum 206, 3700 O'Hara St, Pittsburgh, PA 15213, USA
mlk53@pitt.edu

ABSTRACT

Temperature fluctuations are known to occur in the mixing region of non-isothermal flows, and can cause undesired thermal stresses. This is a concern in certain key components for next generation high temperature gas cooled reactors. One such reactor concept is the very high temperature gas reactor (VHTR), which uses helium as the primary coolant. In the lower plenum of such reactors, the coolant channels mix together and are collectively routed to a gas turbine or hydrogen production facility, and the potential for incomplete mixing is a concern. The objective of this study is to gain insight into the thermal loading conditions expected in the VHTR lower plenum. To analyze the lower plenum mixing behavior, an experimental study of the interactions of three non-isothermal parallel round jets is conducted. A cold jet is surrounded on either side by two hot jets with air as the working fluid. A flat polycarbonate plate is mounted parallel to the axial direction of the jets, with the top edge of the plate directly behind the outlets of the jets. In this configuration the downstream thermal mixing of the jets can be studied. Infrared temperature measurements of the plate surface enable characterization of the thermal forcing function. In general, the highest fluctuations occur in the plane common to the three jet axes. These fluctuations are also increased when the neighboring jets are at the same velocity. The research completed here represents the first step enabling confident predictions of the thermal loading in the VHTR lower plenum. These experiments are intended to serve as validation data for fundamental and applied thermal mixing simulations.

KEYWORDS
lower plenum; parallel triple jet; round jet; thermal loading; very high temperature reactor

1. INTRODUCTION

In both existing and next generation nuclear reactor designs, the mixing of hot and cold fluids at the outlet of the reactor core is of major concern due to the induced high thermal fluctuations in this area. These temperature fluctuations can cause severe high cycle thermal fatigue over the course of the nuclear reactor's operational lifetime and are known as thermal striping. Over the course of a reactor's lifespan, the effects of thermal striping can jeopardize the structural integrity of nuclear reactor cores and their adjacent coolant lines. Thermal striping is especially problematic in the Generation IV very high temperature gas reactors (VHTR), which employ helium as a coolant. Helium has several distinct advantages over water, of which include a higher heat capacity, which implies higher thermal fluctuations than modern pressurized water reactors (PWRs). Unlike modern PWRs which have water flow upward through the reactor, the helium coolant flows vertically downward through the VHTR core. The helium extracts heat throughout the core before mixing in the lower plenum, much like an array of impinging jets, and then exits the lower plenum through one single outlet. The mixing that takes place in the lower plenum is caused by the non-uniform heating of the helium in the reactor core and can have up to 300-400 K differences in jet outlet temperatures

which are flowing in parallel to the internal wall structures of the VHTR core. Research on thermal fatigue is primarily focused on the thermal-hydraulic, thermal-mechanics, and material science aspects of design. In this paper, the thermal-hydraulic and thermal-mechanics aspects are coupled, and the results are to promote future research in the area of materials science.

The issue of thermal striping in nuclear reactor cores was first introduced as a major cause of structural fatigue in the early 1980's. Lloyd and Wood [1] first presented the issue in their analysis on the initiation and subsequent propagation of surface cracks in a stainless steel section subjected to high frequency thermal shocks. Thermal shocking is defined as the condition in which the surface temperature change has occurred before the effects have penetrated significantly through the component wall [2]. With continuous thermal shocks, the thermal striping experienced by internal wall components becomes more severe over time. For gas cooled and fast reactors at high temperatures (over 500 ˚C), the primary mode of material failure is creep with fracture becoming more of a concern in larger components. However, with higher allowable coolant temperatures in these reactor types, fracture is generally less of a concern since there is no need for pressurization to prevent boiling. This allows for the reactor to stay online for a longer period of time, while also subjecting it to more thermal shocking. With reactors like the VHTR being online for decades at a time, the potential for creep in internal wall structures becomes far more likely.

Previous experimental and numerical investigations have modeled a confined series of three parallel jets by themselves, or with interaction from solid components replicating basic geometric components. Tokuhiro and Kimura [3] conducted experiments with a triple slot jet configuration with a central cold jet (non-buoyant) and a hot jet on either side (considered buoyant), with an additional single jet used as a reference. Water was used as the fluid medium. The slot jets discharged into an enclosed tank and a thermocouple tree was used to measure temperatures in a 2D plane downstream from the jets. Three regions of flow were studied, the first being termed the "entrance" region where temperature was considered constant (negligible increase in cold jet temperature and decrease in hot jet temperature). The second area, known as the "convective mixing" area denotes the area where the temperature increase/decrease is significant. The area of study furthest downstream was considered the "post mixing" region where the temperature assumes an asymptotic trend [3]. A similar numerical study was conducted by Cao et al [4] involving the same parallel triple slot jet configuration with water as the working fluid. The thermal fluctuations from a parallel triple slot jet were modelled using ANSYS Fluent software with large eddy simulation (LES). The temperature fluctuations were analysed as a function of velocity field and Reynolds number from the computed temperature and velocity. The amplitude and frequency data were determined from monitored positions in the free stream of the jets. It was concluded that vortices are closely related with the temperature fluctuation phenomenon as expected, and that by increasing the Reynold's number, the mixing of hot and cold flows is delayed while the convective mixing region is enlarged. Cao et al.'s numerical results are in good agreement with those determined experimentally by Tokuhiro and Kimura.

Similar experimentally-validated numerical studies have been conducted by Nishimura et al. [5] and Kimura et al. [6]. Nishimura et al. focused on numerical simulations involving the low Reynolds number turbulent stress and heat flux equation models (LRSFM) and the standard two-equation k-ε turbulence models. The LRSFM model simulated the experimental results with respect to oscillatory motion and mean temperatures of the flow profile. It was concluded that k-ε could not reproduce the oscillating motion of the jets. The roll up motion of the hot jets, in which they "roll-up" and mix with the cold jet via oscillatory motion, proved to be infeasible for this turbulence model. From the LRSFM model, it was revealed that the periodic oscillation was most apparent in the region where the jets merged and formed a composite jet, referred to previously as the "convective mixing" area. Downstream of the convective mixing area, in the post mixing area, the temperature difference was mainly reduced by turbulent mixing.

Several experimentally-validated numerical studies have also been performed to analyse the interaction of multiple parallel jets with solid components replicating basic geometric components. One of the most

notable of these studies is that performed by Kimura et al. [7] in which a sodium experiment was utilized with parallel jets flowing across a stainless steel wall. The purpose of this study was to determine an evaluation method for the heat transfer coefficient in which a transfer function of the temperature fluctuation between the fluid and wall can be used. The contours of time-averaged temperature and fluctuation intensity in the higher discharged velocity case was found to be similar to those in the lower velocity case.

By assuming a constant heat transfer coefficient in the plate, a simple design method was produced for thermal striping. The evaluation method for the heat transfer coefficient was found to accurately predict the temperature fluctuation in the wall from the fluid temperature. From this validation, the heat transfer coefficients were found as a function of the Peclet number based on the discharge velocity in the wall jet configuration. The heat transfer coefficients were independent of the discharge velocity profile for both isovelocity and non-isovelocity cases. Tenchine et al. [8] have since provided numerical evidence to validate that air can be used as a simulant fluid to properly simulate sodium mixing jet characteristics in the fluid. By using the large-eddy simulation and k-ε model, the experimental data provided by Kimura et al. [7] was validated numerically. It should be noted that this conclusion was met without considering the transfer function of temperature fluctuations to a structure. While the work performed by Tenchine et al. did not include a structural response function in their numerical analysis, several other studies have. Other numerical studies involving thermal mixing induced by multiple parallel jet configurations on solid components include work done by Jones et al. [9] with an impulse response method and Kasahara et al. [10] with a frequency response function. Both of these studies provide response functions for calculation of the thermal stresses induced by fluid temperature fluctuations for use in fatigue strength analysis. Outside of the flat plate configuration, work has also been conducted by Lee et al [11] for thermal mixing in a mixing tee configuration akin to the thermal striping in simplified piping models of light water reactor (LWR) tee junctions.

Much effort has also been given to understanding the flow physics involved with turbulent jets. Particular emphasis has been given to slot jets as they pertain to liquid metal fast reactors. Notable work in this area has been done by Spall et al [12] and Choi et al [13]. There is far less analysis regarding the flow behaviour of multiple turbulent circular jets, such as those seen at the outlet of the VHTR core in the lower plenum. Zhang et al [14] performed a numerical investigation of the turbulent circular wall jet with both flow and mixing characteristics. The LES and two separate RANS models with enhanced wall functions were used. It was determined that LES provided better agreement with experimental data, however some under prediction was present for the span wise velocity profiles away from the jet centerline. The subject of multiple turbulent circular jets is of great significance in the study of the VHTR lower plenum. Further understanding of the flow characteristics and heat transfer interaction with an adjacent parallel wall is of particular interest. Therefore, an experimental model of the triple parallel round jet to parallel wall study is herein presented and compared to existing studies for slot jets, and to a lesser extent, the available studies on circular jets.

2. EXPERIMENT

2.1 Experimental Facility

The experimental facility allows for a series of three round jets to flow parallel to an adjacent wall. Figure 1 provides a visual representation of the experimental setup.

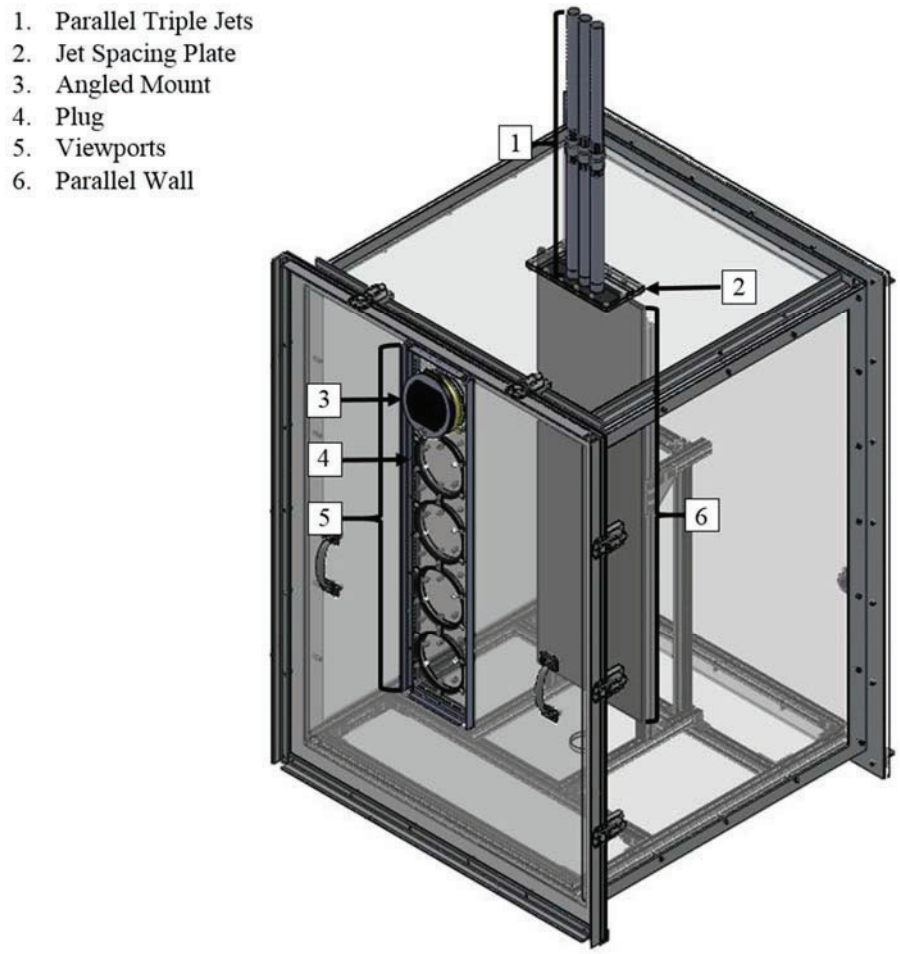

Figure 1: Isometric view of triple jet test section

The facility includes a 73.66 cm x 76.20 cm x 106.68 cm enclosed test section with three parallel round jets whose outlets are located on the top surface of the test section. At the bottom of the test section, a 5.08 cm line allows air to exit the facility. The test section's outer support frame includes rubber feet to dampen any type of unwanted vibrational response from the surrounding environment. The three parallel jets are fixed vertically via a structural support frame and are connected to a corresponding external temperature and flow control skid. The temperature and flow control skid includes two separate heaters for the two outermost jet lines and a heat exchanger for the center jet line with flow for all three lines produced by a blower. An additional system heat exchanger is included to regulate unwanted increases in jet temperatures from downstream mixing and re-entry of the flow in the blower. Additional details regarding the temperature and flow control skid are previously detailed in [15] which also utilizes air as the working fluid. The exit line at the bottom of the test section returns to the temperature and flow control skid. The jets themselves consist of two 30.48 cm pipes with internal diameters of 2.22 cm connected via a custom coupling. Inside each coupling is a honeycomb insert for flow straightening and improved uniform turbulence quantities. The honeycomb flow straighteners are composed of Somos® NanoTool, which has a glass transition temperature of 88.89 ˚C. The honeycomb straightener length is such that L/D_{hyd} = 20, where L is the length of the flow straightener and D_{hyd} is the hydraulic diameter of a singular hexagonal channel. Inside the test section is the parallel wall of dimensions 27.94 cm x 96.52 cm x 0.95 cm which is fixed via a structural support frame. The parallel wall is composed of polycarbonate and is painted with Krylon 1602 paint with an emissivity (ϵ) of 0.95 [16]. The thermal conductivity of the polycarbonate plate is 0.19 W m^{-}

[1] K^{-1} and has a melting temperature in the range of 230-260 ˚C. The parallel plate is composed of polycarbonate due to its optimal thermal properties regarding the proposed temperatures the plate is subjected to. Its low thermal conductivity prevents "smearing" of the temperature profiles on the front surface of the plate, enabling a better quantification of the thermal loading functions themselves, and not an attenuated version of them.

2.2 Experimental Parameters

The three jets consist of a center cold jet with an adjacent hot jet on either side. The hot jets are consistently set to the same temperatures and flow rates for each test case. The test cases are categorized by the velocity ratio (R) between the cold and hot jets:

$$R = \frac{V_C}{V_H} \tag{1}$$

where V_C is the velocity of the cold jet and V_H is the velocity of the hot jet. In this ratio, V_H refers to the velocity of a single hot jet, not the cumulative velocity of both hot jets. For each test case, the temperature difference between the jets is 22.2 °C, providing for a sufficiently high temperature gradient between the hot and cold jets for clear temperature profile visualization. Since the area of each jet is the same, and the absolute temperature range is fairly small, the velocity ratio can be calculated using the experimentally specified volumetric flow rates. The test cases are presented in Table 1.

Table 1: Experimental triple jet configurations

Case Name	*Hot Jet*			*Cold Jet*			ΔT (°C)	R
	$\dot{V}_H$ (m^3/min)	Re_H	T_H (°C)	$\dot{V}_C$ (m^3/min)	Re_C	T_C (°C)		
Case 1	1.133	15432	44.7	0.566	7716	22.5	22.2	0.5
Case 2	0.566	7716	45.6	0.566	7716	23.3	22.2	1.0
Case 3	0.377	5144	47.8	0.566	7716	25.6	22.2	1.5

The plate spacing from the jets, herein defined as 'δ', provides another experimental parameter of interest. The plate spacing, "δ", is defined in terms of the number of hydraulic diameters the plate is from the axial centerline of the three jets. For this preliminary study, the plate is fixed directly tangent to the outlets of the jets (δ = 0.5). This provides the most apparent temperature profile of the jet potential cores possible, with minimal effects from the ambient air of the tank, since there is no free stream gap between the jet flows and the plate. The spacing of the jets relative to one another, herein defined with the variable 'S', also influences the mixing on the plate surface. The non-dimensional axial direction Y* is defined as Y*=Y/S where the non-dimensionalized axial direction Y* and distance S can be seen in Figure 2 and Figure 3, respectively. The minimum center-to-center spacing at the outlets of the jets, which is based on a scaled mock-up of the General Atomics gas turbine modular helium reactor (GT-MHR) [17], is S = 3.13 cm. This minimal spacing was chosen for this preliminary analysis.

2.3 Experimental Methods

The volumetric flow of the individual jets are held constant by the temperature and flow control skid's automated valves after the jet temperatures reach steady state [15]. The jet outlet temperatures are determined experimentally by placing a type-T thermocouple with a resolution of +/- 0.5 °C at the outlet of each jet. A FLIR SC5000 IR camera with a resolution of +/- 1.0 °C is used to acquire the temperature

signatures induced by the jets on the parallel plate. The test section walls are composed of 1.11 cm thick polycarbonate and have poor infrared transmittance in the wavelength spectrum of the IR camera (2.1-5.1 μm). For this reason, a FLIR 4 in Infrared (IR) viewport (model IRW-4C) is incorporated, which includes a lens composed of calcium fluoride with a maximum operating temperature of 260 °C. The camera is placed approximately 55.88 cm from the front surface of the parallel plate. To avoid reflection of the camera on the window, the window is mounted at a 10° angle with respect to the camera lens. Additionally, a shroud is placed between the camera lens and the viewport which eliminates any incident radiation. Accommodation for 5 viewports were created on the front surface of the test section with a center-to-center distance of 15.24 cm for each adjacent viewport. The angled mount and IR window can be placed in any of these five viewports with the remaining viewports sealed with plugs. Each viewport allows for a view of the parallel plate with an image approximately 7.7 jet diameters in height, and 6.0 jet diameters in width of the parallel plate. The viewport design can be better visualized in Figure 3.

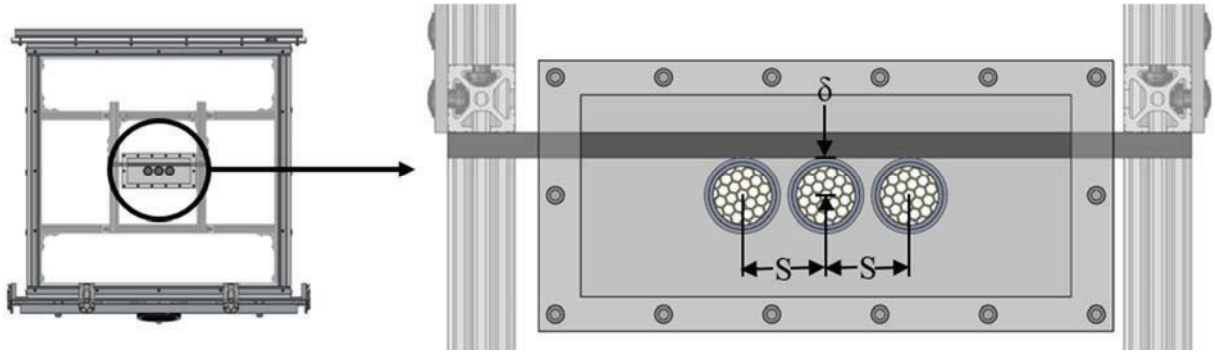

Figure 2: Top view of triple jet test section with confining wall

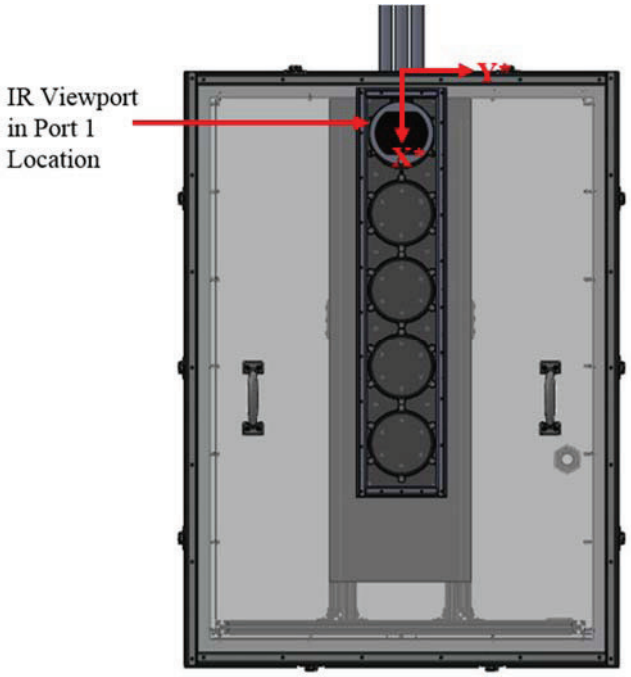

Figure 3: Front view of test section and IR viewports

For the present study, only the top three viewports are utilized. The overlap between the three viewports in the X-direction has been determined, providing for one coherent study of the thermal loading on the plate from the outlets of the triple jet configuration. For this study the non-dimensionalized X* axis is used as

seen in Figure 3, where $X^*=X/D_{hyd}$ where D_{hyd} is the hydraulic diameter of an individual jet. The current study provides insight into the important flow physics for non-isothermal mixing. Therefore, the individual temperature profiles captured by each viewport are analyzed for each proposed test case.

3. RESULTS

3.1 Temperature Profiles

The temperature profiles captured by the IR camera at each viewport for each case in Table 1 can be found in Figure 4. The temperature scaling of each figure is held constant to enable qualitative and quantitative comparisons.

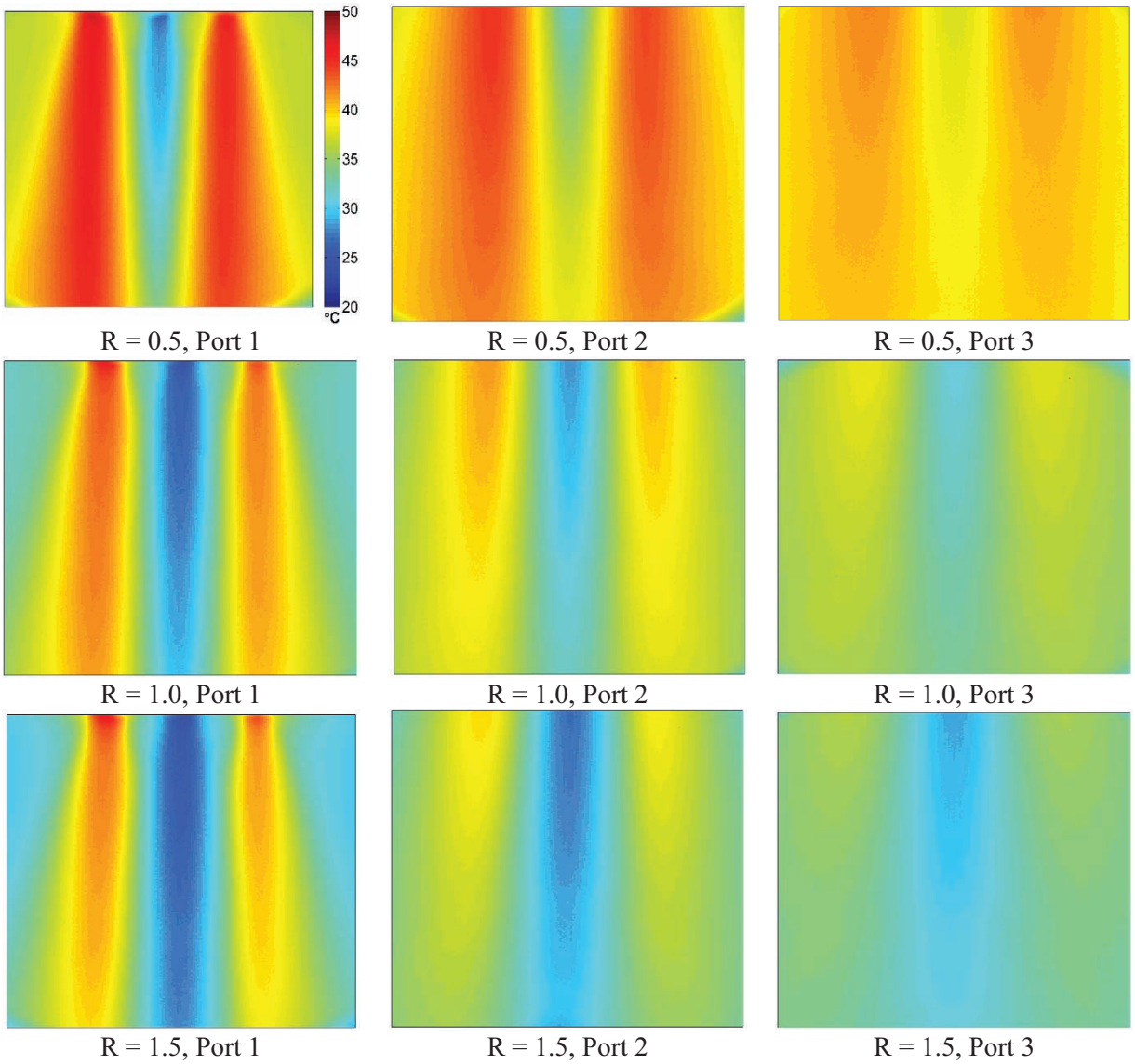

Figure 4: Contours of triple jet-induced temperature fields across parallel wall. Approximate size of each image is 13.4 cm x 17.1 cm.

From Figure 4, it is clear that the most apparent difference in the surface temperature of the polycarbonate plate is in the R = 0.5 Port 1 temperature field. For this test, the results show the immediate effect of the individual jet flows on the plate surface in the entrance region of the jets, before any notable mixing has taken place. The effect of the velocity ratio is most apparent in this region in that the hot jets dominate the temperature profile seen on the plate and all three jets are clearly defined. The entrance region is easily classified because negligible change in temperature has occurred directly at the outlets of the cold and adjacent hot jets which is in good agreement with the same behavior described in the experiments conducted by Tokuhiro and Kimura [3]. In the corresponding downstream thermal fields for the R = 0.5 case, the convective mixing region becomes more apparent, specifically in Port 2. By the lower half of Port 3, the profile is almost in the post mixing regime with near uniform temperatures across the surface of the plate. The entrance region seen in the R = 1.0 Port 1 case is less clear than in the R = 0.5 Port 1 case, since the velocities are now equal. The "squeezing" experienced by the cold jet becomes slightly less apparent in the isovelocity case Port 2 image. This is due to the isovelocity condition itself, in which the viscous effects are minimized and the differences in physical properties of air at these absolute temperatures (T_c = 24.3˚C and T_h = 46.2 ˚C, for the cold jet and hot jets, respectively) are assumed negligible. Therefore, for the R = 1.0 case, the convective mixing of the jets is now based primarily on the temperature difference between the jets. The post mixing region appears most prominent in the R = 1.0 Port 3 case. In the R = 1.5 case, the cold jet velocity is sufficiently higher than the two adjacent hot jets' velocities such that the cold jet dominates the temperature field seen on the plate, even as far downstream as Port 3. Thus the squeezing experienced by the cold jets due to the hot jets in the R = 0.5 case is now reversed, and in the R = 1.5 case the cold jet is instead beginning to push out the adjacent hot jets in Port 2. Interestingly, the thermal mixing behavior seen in the R = 0.5 Port 3 case seems sufficiently mixed, characteristic of the post mixing region, similar to that of the R = 1.0 Port 3 temperature field. As expected, the main difference between the post mixing regions in these two cases are the absolute temperatures seen in each. The R=0.5 case consists of a total volumetric flow between the three jets of 2.832 m^3/min while that of the R=1.5 case is 1.321 m^3/min. For this reason, the R=0.5 case should have a higher post mixing temperature in the plate due to the significant increase in mass flux of the fluid and increased heat transfer through the plate. The 9 plots in Figure 4 provide a comprehensive example of the three mixing regions previously described by Tokuhiro and Kimura [3]. The mixing regions are visualized for the three proposed velocity ratios (R = 0.5, 1.0, 1.5) with a constant temperature difference at the outlets of the jets.

3.2 Jet-Induced Temperature Peaks

Line traces of the temperature data were utilized in X*=2 increments in the downstream non-dimensionalized X*-direction (as depicted in Figure 3) for each temperature field. A total of 10 line traces were evaluated accounting for a range of X* values between X*=2-20 downstream. As an example, a visualization of the line traces and the corresponding temperatures are seen in Figure 5 for the R = 1.0 (isovelocity) Port 1 case with the X* = 2, 4, 6 line traces.

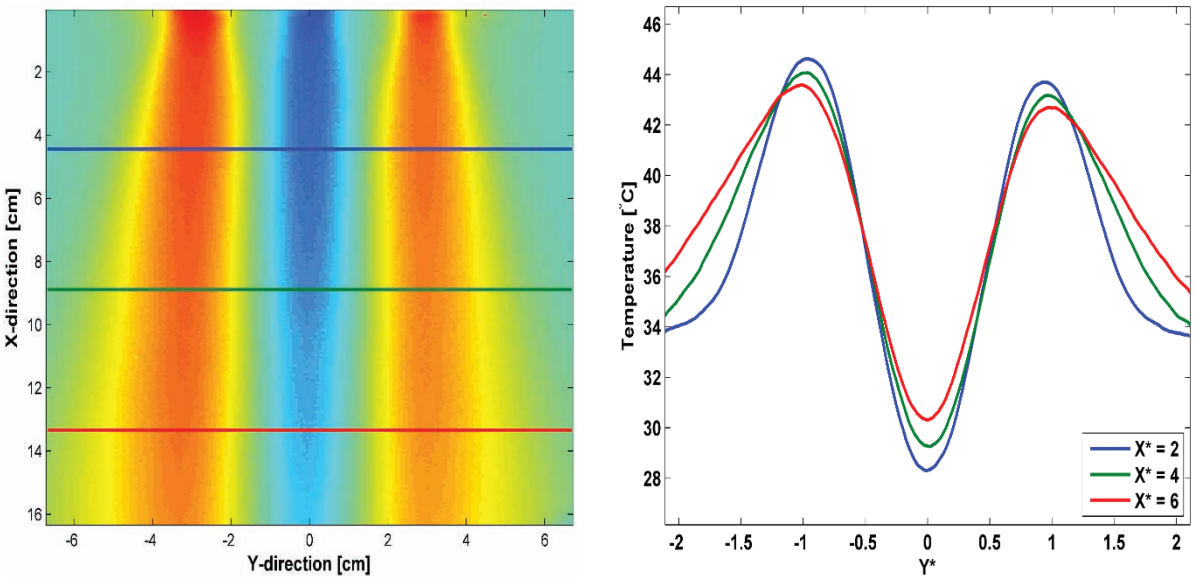

(a) (b)

Figure 5: (a) Case 1, Port 1 temperature field with imposed line traces (b) Case 1, Port 1 polycarbonate plate surface temperatures

As previously stated, the X*-direction length scale for each viewport is relative to the overall length downstream. The line traces provide an array of temperatures along the width of the plate, in the Y*-direction (as depicted in Figure 3). For an improved understanding of the characteristic behavior of the line traces, the asymmetry of each trace was resolved by averaging each line trace about its center-most point, the cold jet center. The maximum relative asymmetric error for two individual symmetrically averaged pixels was found to be 7.8, 3.5, and 4.1% for Case 1, 2, and 3, respectively. Additionally, the notable relative asymmetric error for each case was found on the outside of the hot jets where the relative asymmetric error inside the three jets (Y* = -1 to Y*= 1) was less than 3% for each case. This implies that the slight asymmetry in the jets for each test case was acceptable and the majority of the asymmetry was due to dissipation outside of the mixing area of the triple jet configuration.

Additionally, the non-dimensionalized temperature, θ, is introduced such that the minor differences in the hot and cold jet temperatures for each test case are now considered negligible when comparing the three proposed test case in Table 1. The non-dimensionalized temperature is introduced according to

$$\theta = \frac{T - T_C}{T_H - T_C} \tag{2}$$

Where T is the temperature at a given pixel, T_H is the maximum hot jet outlet temperature, and T_C is the cold jet outlet temperature. The line temperatures for the X*=2-20 distances downstream for each case can be seen in Figure 6 as

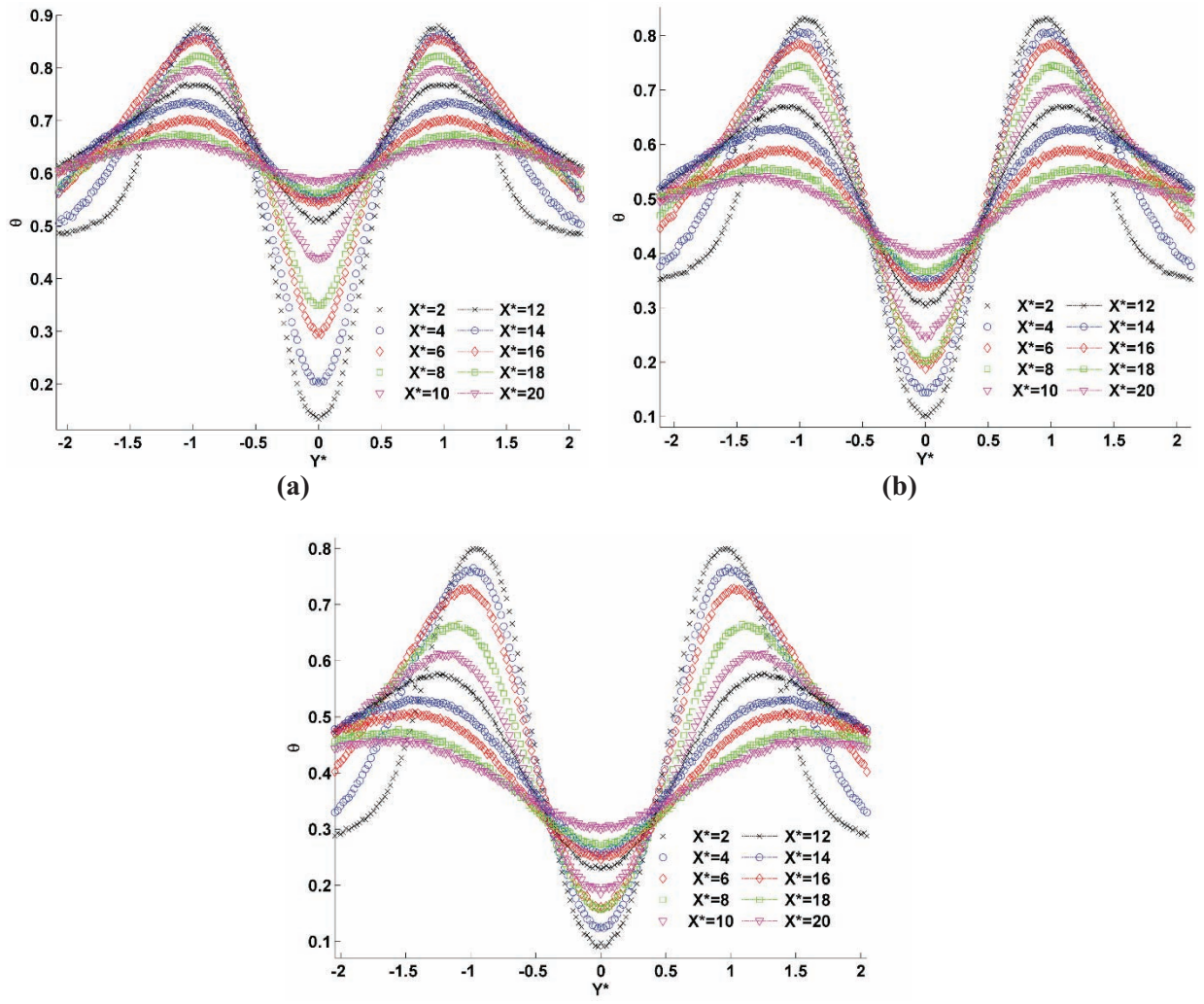

Figure 6: Temperature line profiles for (a) Case 1 (b) Case 2 (c) Case 3

In Figure 6(a), Case 1 shows the effect of the hot jets' dominance over the line temperature profiles with increasing X* intervals downstream. This is due to the R=0.5 parameter in which the mass flux from the hot jets dominates the temperature profile seen on the plate. The line temperatures become increasingly horizontal with downstream distance in the X*-direction implying that the temperature profile on the plate is becoming more evenly mixed. The same could be said for Case 2 and 3 in Figure 6(b) and (c), however in Case 1 the line temperature horizontal averages are higher than Case 2, and likewise, the horizontal averages in Case 2 are higher than Case 3. Additionally, the "spreading" of the jets in the Case 1 and Case 3 line temperature plots show inverse behavior. In Case 1 where the hot jets dominate, the cold jet "spreads" far more with downstream distance as the line temperatures reach thermal equilibrium downstream. The opposite behavior is seen in Case 3 where the hot jets spread more aggressively downstream where the cold jet mass flux dominates. These aggressive shifts in surface temperatures along the plate with downstream distance suggest areas of potential thermal striping concern.

The analysis found in Figure 6 allows for evaluation of the maximum temperature of the hot jets relative to the X* and Y*-direction on the plate surface. The location of the maximum temperature of each downstream line trace for each case are provided in Figure 7

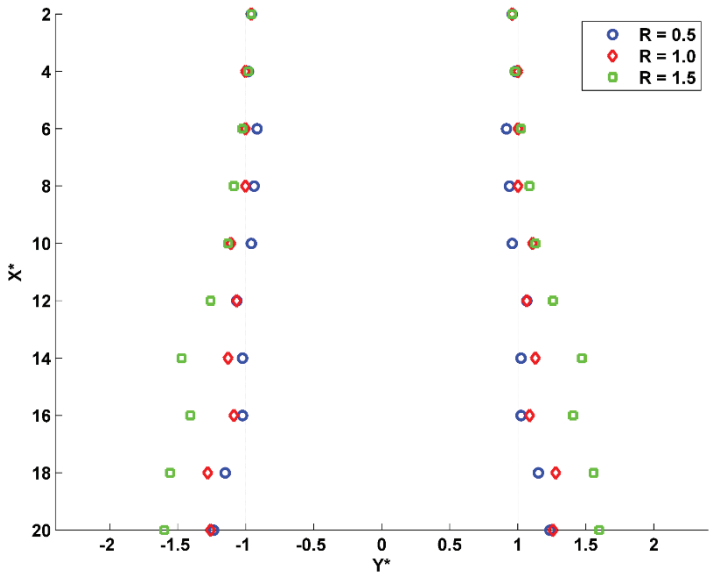

Figure 7: Peak temperature location for each line trace

For the case with the highest hot jet velocity (R = 0.5), the peak temperature of each line trace was relatively close to the jet center lines. As the hot jet velocities were reduced for the R = 1.0 and R = 1.5 cases, the peak temperatures gradually move position further outside from the two jet centerlines, as the cold jet flow contributes more to the mixing taking place on the surface of the plate. Also worth noting is the downstream behavior of each case. For each case, the Port 2 line traces provide peak temperatures that were slightly further outside than that of the Port 1 peak temperatures. The same comparison can be made for the peak temperatures seen in Ports 2 and 3, in that the peak temperatures are even further out from the jet centerlines. This moving peak temperature away from the hot jet center lines shows the dissipation in the heated flow across the plate in the Y*-direction. This implies that the heat is being conducted more outwardly along the surface of the plate as the flow moves downstream and is highly dependent on the velocity ratio between the center cold jet and outer hot jets.

4. CONCLUSIONS

The temperature fields provide comprehensive examples of the three regions of flow experienced by the triple round jet to parallel wall configuration. These temperature profiles are in good agreement with profiles determined using a similar slot jet to parallel wall configuration in previous studies [3], [4], [7], [8]. The spreading of the temperature profiles for each case and the moving peak temperature found as a function of the line traces across the plate and downstream location hint at the possibility of an empirically determined probability function of crack propagation in the plate as induced by thermal striping. Future research will look more closely at the movement of the line temperature profiles and peak temperature downstream along the plate and will utilize additional temperature differences, as well as plate spacings and jet spacings that are geometrically comparable to those seen in the scaled version of the lower plenum of the VHTR core. This study provides for a preliminary view of the work to come in determining the thermal loading as a function of the jet Reynolds numbers, the temperature difference between the jets, and the plate position. These studies provide for useful insight in preventing thermal striping in the internal structural walls of the VHTR lower plenum and will be utilized in future work in material analysis of structural integrity in the VHTR core.

ACKNOWLEDGEMENTS

This research is being performed using funding received from the DOE Office of Nuclear Energy's Nuclear Energy University Programs.

REFERENCES

1. Lloyd, G.J., Wood, D.S., "Fatigue Crack Initiation and Propogation as a Consequence of Thermal Striping", International Journal of Pressure Vessels and Piping, **8**, pp. 255-272 (1980).
2. Clayton, A.M., "Thermal Shock in Nuclear Reactors", *Progress in Nuclear Energy*, **12**(1), pp. 57-83 (1983).
3. Tokuhiro, A., Kimura, N., An experimental investigation on thermal striping mixing phenomena of a vertical non-buoyant jet with two adjacent buoyant jets as measured by ultrasound Doppler velocimetry, *Nuclear Engineering and Design*, **188** pp. 49-73 (1999).
4. Cao, Q., Lu, D., and Lv, J., "Numerical investigation on temperature fluctuation of the parallel triple-jet", *Nuclear Engineering and Design*, **249**, pp. 82-89 (2012).
5. Kimura, N., Nishimura, M., Kamide, H., "Numerical study on mixing of oscillating quasi-planar jets with low Reynolds number turbulent stress and heat flux equation models", *Nuclear Engineering and Design*, **202**, pp. 77-95 (2000).
6. Nishimura, M., Tokuhiro, A., Kamide, N., "Study on Convective Mixing for Thermal Striping Phenomena", *JSME International Journal*, **45**(3), (2002).
7. Kimura, N., Miyakoshi, H., Kamide, H., "Experimental investigation on transfer characteristics of temperature fluctuation from liquid sodium to wall in parallel triple-jet", *International Journal of Heat and Mass Transfer*, **50**(9-10), pp. 2024-2036 (2007).
8. Tenchine, D., Vandroux, S., Barthel, V., Cioni, O., "Experimental and numerical studies on mixing jets for sodium cooled fast reactors", *Nuclear Engineering and Design*, **263,** pp. 263-272, (2013).
9. Jones, I.S., Lewis, M.W.J., "An Impulse Response Model for the Prediction of Thermal Striping Damage", *Engineering Fracture Mechanics*, **55**(5), pp. 795-812 (1996).
10. Kasahara, N., Takasho, H., Yacumpai, A., "Structural response function approach for evaluation of thermal striping phenomena", *Nuclear Engineering and Design*, **212**, pp. 281-292 (2002).
11. Lee, J.I., Hu, L.W., Saha, P., Kazimi, M.S., "Numerical analysis of thermal striping induced high cycle thermal fatigue in a mixing tee", *Nuclear Engineering and Design*, **239**(5), pp. 833-839 (2009).
12. Spall, R., Anderson, E., Allen, J., "Momentum Flux in Plane, Parallel Jets", *Journal of Fluids Engineering*, **126**(4), pp. 665 (2004).
13. Choi, S., Kim, S., "Evaluation of Turbulence Models for Thermal Striping in a Triple Jet", *Journal of Pressure Vessel Technology*, **129**, pp. 583-592 (2007).
14. Zhang, S., Law, A., Zhao, B., "Large eddy simulations tubrulent circular wall jets", *International Journal of Heat and Mass Transfer*,. **80**, p. 72-84 (2015).
15. Landfried, D.T., Goclano, B., Kimber, M. "Design of a scaled non-isothermal experimental facility for studying the thermal hydraulics of the lower plenum of a prismatic VHTR", *Proceedings of the 15th International Topical Meeting on Nuclear Reactor Thermal Hydraulics (NURETH-15)*, Pisa, Italy, May 12-17, 2013 (2013).
16. NASA jet Propulsion Laboratory Web Site, http://masterweb.jpl.nasa.gov/reference/ paints.htm (1997).
17. McCreery, G., Condie, K., "Experimental Modeling of VHTR Plenum Flows During Normal Operation and Pressurized Conduction Cooldown", INL/EXT-06-11760, September, 2006.